TASK QUARTERLY 11 No 3, 263–271

NUMERICAL SIMULATIONS OF SLOW MAGNETOSONIC STANDING WAVES IN A TWO-DIMENSIONAL HOT SOLAR CORONAL SLAB

RAFAŁ OGRODOWCZYK[1] AND KRZYSZTOF MURAWSKI[2]

[1]*Institute of Mathematics and Computer Sciences, The State University in Chełm, Pocztowa 54, 22-100 Chełm, Poland*
rogrodow@pwsz.chelm.pl

[2]*Group of Astrophysics and Gravity Theory, UMCS, Radziszewskiego 10, 20-031 Lublin, Poland*

(Received 8 January 2007; revised manuscript received 23 March 2007)

Abstract: We consider impulsive excitation of slow magnetosonic standing waves in a two-dimensional hot solar coronal slab. Results of numerical simulations have revealed that initially launched pulses trigger mainly fundamental slow mode and its first harmonic, depending on the pulses' spatial location. Our parametric study has shown these slow standing waves to exhibit wave periods of about 13min. The slow standing waves are accompanied by fast modes simultaneously present in the system.

Keywords: Sun, solar corona, MHD oscillations

1. Introduction

It has been verified through observations that the solar corona consists of myriads of coronal loops which are able to sustain oscillations (Nakariakov and Verwichte [1]). Observations from the SUMER SOHO/EIT and TRACE/EUV have suggested that loop oscillations are often triggered impulsively by micro- or sub-flares near a loop's foot point and are attenuated over several wave periods (Wang *et al.* [2]). Apart from propagating standing wave modes, fast kink (Aschwanden *et al.* [3], Wang and Solanki [4]) and slow (Wang *et al.* [5]) magnetosonic waves have been observed in coronal loops. As wavelengths of these standing waves are determined by a loop's length, we can estimate wave periods with given phase speeds (Roberts *et al.* [6]).

Recently, slow standing waves have been discussed theoretically by several authors. In particular, Mendoza-Briceñ*o* *et al.* [7] have presented results of numerical calculations describing the response of coronal plasma to micro scale heating pulses in a magnetic loop. In particular, they have studied the effects of energy input

pulses injected randomly near the two foot points of a semi-circular loop. They have found that successive random pulses are capable of maintaining the plasma's average temperature at typical coronal values. In another study, Nakariakov *et al.* [8] and Tsiklauri *et al.* [9] have demonstrated that an impulsive energy released in a coronal loop excites the second spatial harmonic. The considered model included the effects of gravitational stratification, heat conduction, radiative losses, external heat input and the Braginskii bulk viscosity. An extensive review of longitudinal intensity fluctuations observed in coronal loops has been presented by De Moortel *et al.* [10].

Several attenuation mechanisms of slow waves have been proposed: wave leakage into the chromosphere (Ofman [11], Van Doorsselaere *et al.* [12]), lateral wave leakage due to the curvature of loops (Roberts [13]), phase mixing (Nakariakov *et al.* [14], Ofman and Aschwanden [15]), resonant absorption (Ruderman and Roberts [16]) and non-ideal MHD effects (Roberts [13]). Ofman and Wang [17] have found that thermal conduction leads to rapid damping of slow standing waves, with a less significant contribution from compressive viscosity. Ofman *et al.* [15] have shown that a nonlinear steepening of slow waves leads to their enhanced dissipation. Nakariakov *et al.* [18] have inferred that dissipation and stratification are the main factors influencing the slow evolution of waves. De Moortel *et al.* [19] have deduced that thermal conduction may account for the observed damping times. Selwa *et al.* [20] have performed parametric numerical studies of slow standing waves in the limit of one-dimensional approximation, the model they have developed is seriously flawed. Its main disadvantage is that it takes into account slow magnetosonic waves only, neglecting the presence of fast magnetosonic and Alfvén waves in the system. As a consequence, the model excludes the possibility of slow wave generation either through a linear coupling process with fast waves or through nonlinear ponderomotive effects exerted by an Alfvén wave.

The aim of this paper is to generalize the study of Selwa *et al.* [20]. The generalization is based on taking into account two-dimensional geometry to explain excitation of slow magnetosonic waves in solar coronal loops. We have found that the presence of a fast wave is an important factor in generating standing slow waves. A system in which Alfvén waves are present remains to be studied in the future.

The numerical model is described in the following section. Numerical results are presented in Section 3. This paper is concluded with a summary of the main results in Section 4.

2. The numerical model

We describe coronal plasma by the time-dependent ideal MHD equations:

$$\frac{\partial \varrho}{\partial t} + \nabla \cdot (\varrho \boldsymbol{V}) = 0, \tag{1}$$

$$\varrho \frac{\partial \boldsymbol{V}}{\partial t} + \varrho (\boldsymbol{V} \cdot \nabla) \boldsymbol{V} = -\nabla p + \frac{1}{\mu} (\nabla \times \boldsymbol{B}) \times \boldsymbol{B}, \tag{2}$$

$$\frac{\partial p}{\partial t} + \nabla \cdot (p \boldsymbol{V}) = (1-\gamma) p \nabla \cdot \boldsymbol{V}, \tag{3}$$

$$\frac{\partial \boldsymbol{B}}{\partial t} = \nabla \times (\boldsymbol{V} \times \boldsymbol{B}), \tag{4}$$

$$\nabla \cdot \boldsymbol{B} = 0, \tag{5}$$

where ϱ is mass density, $\boldsymbol{V}$ is flow velocity, $\boldsymbol{B}$ is magnetic field, p is gas pressure, μ is magnetic permeability and $\gamma = 5/3$ is the adiabatic index.

In the above equations, we have neglected the effect of gravity and non-ideal plasma, which is not entirely justifiable physically. Indeed, Mendoza-Briceñ*o et al.* [21] have found that stratification results in a 10%–20% reduction of the wave-attenuation time compared to non-stratified loop models due to increased dissipation by compressive viscosity due to gravity.

2.1. The slab equilibrium

We limit our discussion to a two-dimensional magnetically structured atmosphere. As the plasma quantities are assumed to be independent of the spatial coordinate y, $\partial/\partial y = 0$, and $V_y = B_y = 0$ the Alfvén wave is removed from the system. Additionally, we assume that the initial, unperturbed (*i.e.* equilibrium) magnetic field is directed in the z direction (Figure 1). A coronal slab is approximated by plasma profiles in which inhomogeneity occurs in the x direction only, *i.e.* $\boldsymbol{B}_0 = \big(0,0,B_0(x)\big)$. In particular, we consider a loop in the form of a slab with half-width w, field strength B_i at the center of the slab and mass density $\varrho_\mathrm{i} = r\varrho_\mathrm{e}$, embedded in a magnetic environment of field strength B_e and mass density ϱ_e. Here, r is the loop density contrast, which we set at $r = 10$ (Figure 1). Although the actual behavior of the kink mode in the slab geometry differs from its behavior in the cylinder, (Roberts *et al.* [22]), the slab model consists the ingredient necessary in the study of a complex loop structure.

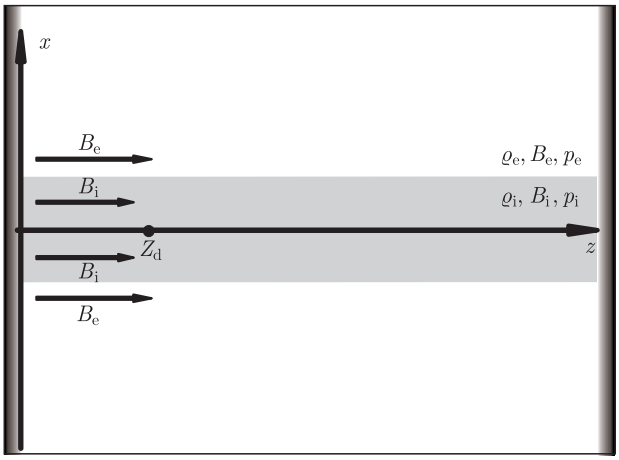

Figure 1. The model's geometry; the Z_d symbol denotes the detector's position

The speeds of the Alfvén, $V_\mathrm{Ai,e}$, and sound, $c_\mathrm{si,e}$, are defined as $V^2_\mathrm{Ai,e} = B^2_\mathrm{i,e}/(\mu\varrho_\mathrm{i,e})$, $c^2_\mathrm{si,e} = \gamma p_\mathrm{i,e}/\varrho_\mathrm{i,e}$, where the 'i' and 'e' indices correspond to the slab and the ambient medium, respectively.

We choose the following parameters: $V_\mathrm{Ae} = 2\mathrm{Mms}^{-1}$, $\varrho_\mathrm{e} = 10^{-15}$ kgm^{-3}, temperature ratio $T_\mathrm{i}/T_\mathrm{e} = 2$, mass density ratio $r = \varrho_\mathrm{i}/\varrho_\mathrm{e} = 10$, Alfvén speed ratio $v = V_\mathrm{Ae}/V_\mathrm{Ai} = \sqrt{10.1}$ and half-width of the slab $w = 2\mathrm{Mm}$. The plasma's β in the ambient medium is defined as $\beta = 2\mu p_\mathrm{e}/B^2_\mathrm{e}$.

The pressure, $p_{\rm e}$, and magnetic field, $B_{\rm e}$, in the ambient medium are then described by the following formula:

$$p_{\rm e} = \frac{1}{\gamma} c_{\rm se}^2 \varrho_{\rm e}, \quad B_{\rm e} = \sqrt{\frac{2\mu}{\beta} p_{\rm e}}, \tag{6}$$

and the corresponding plasma quantities inside the slab are computed from:

$$B_{\rm i} = B_{\rm e} \frac{\sqrt{r}}{v}, \quad p_{\rm i} = p_{\rm t} - \frac{B_{\rm i}^2}{2\mu}. \tag{7}$$

Here, $p_{\rm t}$ denotes the total pressure defined as the sum of the gas and magnetic pressures, *viz.*:

$$p_{\rm t} = p_{\rm e} + \frac{B_{\rm e}^2}{2\mu}. \tag{8}$$

2.2. Perturbations

Perturbations of the slab equilibrium can be triggered in numerous ways. As we are interested in impulsively excited slow waves, we launch a hot pulse in mass density and pressure at $t = 0$, of the following form:

$$[\delta\varrho(x,z), \delta p(x,z)] = [A_\varrho, A_{\rm p}] \exp\left[-\left(\frac{x-x_0}{w_x}\right)^2 - \left(\frac{z-z_0}{w_z}\right)^2 \right], \tag{9}$$

where A_ϱ and $A_{\rm p} = 10\ A_\varrho$ denote relative amplitudes of the initial pulse, (x_0, z_0) – its position, and w – its width. In our studies, we choose and maintain fixed $A_\varrho = 0.5\varrho_{\rm e}$ and $w_x = w_z = L/40 = 1.25\,{\rm Mm}$, where L is the length of the loop, set at $L = 50\,{\rm Mm}$. Notably, the pulse given by Equation (9) triggers magnetosonic waves. In our system, β is small but, as it differs from zero, slow and fast waves are present in the model simultaneously. For low β plasma, the slow and fast magnetosonic waves are weakly coupled and are approximately described by V_z and V_x, respectively. These components of velocity can be described with a linearized Euler Equation (2) (Murawski and Roberts [23]):

$$\varrho \frac{\partial^2 V_z}{\partial t^2} = \frac{B_0}{\mu} \frac{dB_0}{dx} \frac{\partial V_x}{\partial z}, \tag{10}$$

$$\varrho \frac{\partial^2 V_x}{\partial t^2} = \frac{1}{\mu} \frac{\partial}{\partial x} [B_0 \frac{\partial}{\partial x} (B_0 V_x)] + \frac{B_0^2}{\mu} \frac{\partial^2 V_x}{\partial z^2}. \tag{11}$$

If B_0 depends on the x coordinate, V_z and V_x are connected.

3. Numerical results

In our study, we adopted the EMILY numerical code developed by Jones *et al.* [24]. In this code an explicit-implicit algorithm is implemented to solve time-dependent, non-ideal magneto-hydrodynamic equations. We used the explicit algorithm for ideal magneto-hydrodynamic equations. It is second-order accurate in space and time and based on a finite-volume scheme that uses an approximate Riemann solver for hyperbolic fluxes and central differencing applied on nested control volumes for parabolic fluxes arising from the non-ideal terms (*i.e.* resistivity and viscosity).

We solved Eqations (1)–(4) numerically using an Eulerian grid with the x and z dimensions $(-16l, 16l) \times (0, 50l)$, where l is a spatial unit, chosen to be $l = 1\,\mathrm{Mm}$. This Eulerian box was covered by a uniform grid of 400×300 numerical cells. We performed grid convergence studies based on grid refinement to show that the numerical results were unaffected by insufficient spatial resolution.

A time step, Δt, results from the stability (CFL) condition, which basically says that Δt is expressed by a quotient of a cell's width and a maximum value of velocity. It is evaluated by the code. We apply open boundary conditions with zero-gradient extrapolation of all plasma variables allowing a wave signal to leave the simulation region freely. These conditions are applied along the lines given by $x = \pm 16l$.

As the coronal loop is embedded in much denser photosphere, in which waves are essentially reflected, we set the reflecting boundary conditions at $z = 0$ and $z = L$.

3.1. The fundamental mode

Let us first discuss the case of the initial pulse of Equation (9), launched at the point of $x_0 = 0$, $z_0 = L/4$. Spatial profiles of the parallel component of velocity V_z at given moments of time are shown in Figure 2, where we can see that the fundamental mode is excited. These results are confirmed by slices of V_z made along $x = 0$ (Figure 2). They exhibit spatial profiles of $V_z(x = 0, z)$, which are in opposite phases. The profiles of V_z are less regular than in the one-dimensional case considered by Selwa *et al.* [20] (*cf.* their Figure 2). This irregularity is due to the presence of fast magnetosonic waves interacting with slow waves and modifying their profiles.

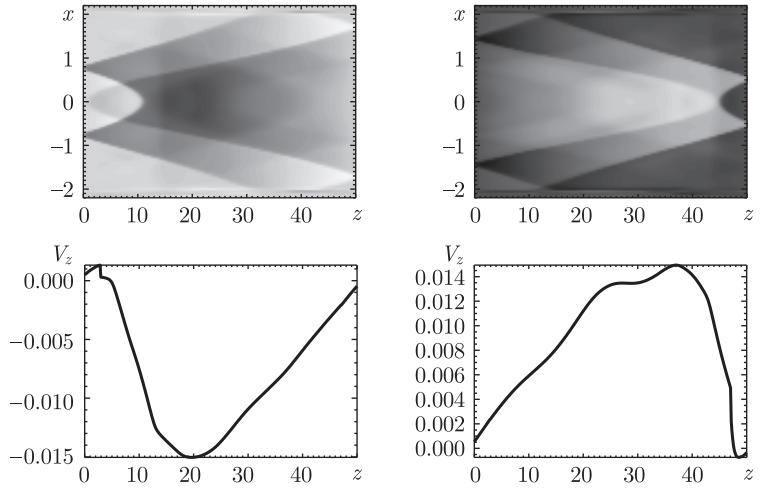

Figure 2. Spatial profiles of the parallel component of velocity V_z (top panels) at $t = 8.78 P_1$ (left panels) and at $t = 9.4 P_1$ (right panels) for the initial pulse position, $x_0 = 0, z_0 = L/4$; slices of V_z drawn along $x = 0$ are shown in the bottom panels

As the pulse's initial amplitude is large, nonlinearity also plays a role in the distortion of a wave signal. Indeed, time signatures of parallel velocity, V_z, and mass density, ϱ_i, collected at $(x = 0, z = L/4)$, can be seen in Figure 3. They are reminiscent of attenuated oscillations. A sign of third-order nonlinearity is noticeable in the right panel of Figure 3, leading to a steepening of the wave's trailing parts.

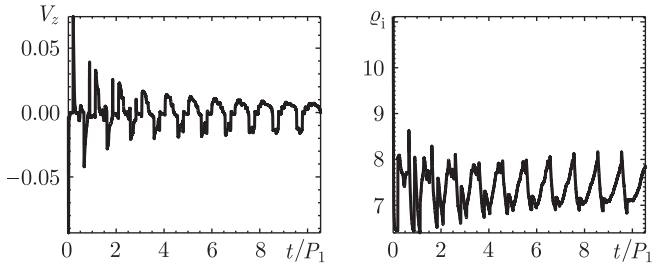

Figure 3. Temporal evolution of parallel velocity, V_z, (left panel) and mass density, ϱ_i, (right panel) collected at $(x=0, z=L/4)$ for the initial pulse position, $x_0=z_0=L/4$

This irregular pattern of time signatures of wave signal (Figure 3) may also result from the presence of fast magnetosonic waves interacting with the slow mode. Spatial profiles of the perpendicular component of velocity, V_x, are shown in Figure 4, reminiscent of the fundamental mode. We can thus conclude that oscillation of slow waves is dominant in the system.

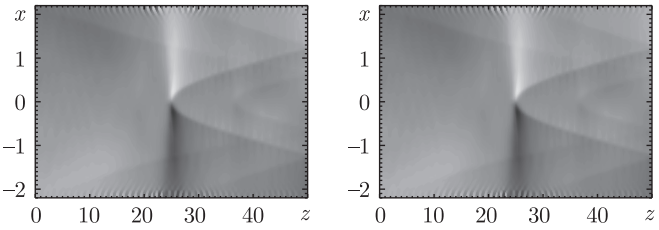

Figure 4. Spatial profiles of the perpendicular component of velocity, V_x, at $t=8.87P_1$ (left panel) and $t=9.38P_1$ (right panel) for the initial pulse position, $x_0=0, z_0=L/4$

The presence of standing waves in a physical system can be determined by the normalized phase shift between oscillations in V_z and ϱ_i, $\delta\phi$. Analytical evaluations have shown that $\delta\phi$ should be equal to a quarter of a wave's period (Nakariakov and Verwichte [1]). We have used an excitation criterion according to which a standing wave is present in the system if $\delta\phi$ departs from 1/4 by 20% (Selwa *et al.* [20]):

$$\frac{1}{4}\cdot 80\% \leq \delta\phi \leq \frac{1}{4}\cdot 120\%\,. \tag{12}$$

According to this criterion, which is fulfilled for $t > t_{\min}$, we have found that the fundamental standing wave is excited at $t \approx 4.3P_1$, where the analytically evaluated period P_1 follows from:

$$P_n \simeq \frac{2L}{n c_{si}}. \tag{13}$$

Here, n is a standing wave number, while $c_{si}=\sqrt{\gamma p_i/\varrho_i}=0.059\,\mathrm{Mm\,s^{-1}}$ denotes the sound speed inside the loop. For these settings, we obtain $P_1=1694.91$s. In the 1D case discussed by Selwa *et al.* [20], fundamental standing waves were excited at $t\simeq 6P_1$. Consequently, we infer that in the 2D case the fundamental sound wave is excited earlier than in the 1D case.

The Fourier spectrum of $V_z(x=0, z=L/4, t)$ is shown in Figure 5. It yields a wave period of 1693.45s, close to the analytically determined value, and reveals the presence of the first harmonic mode, $n=1$, and the $n=3$ harmonic mode. We

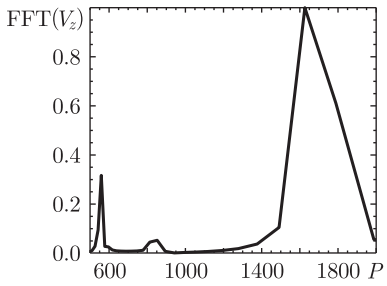

Figure 5. Fourier spectrum of $V_z(x=0, z=L/4, t)$ illustrated in Figure 3, in the range $500 \leq P \leq 2000$s. The Fourier and wavelet analyses (not shown) yield wave period $P_1 = 1693.45$s

infer that the presence of the second harmonic results from the amplitude of the pulse greater than in the one-dimensional case (Selwa *et al.* [20]), which perturbs the regularity of evolution of slow standing waves.

3.2. The first harmonic mode

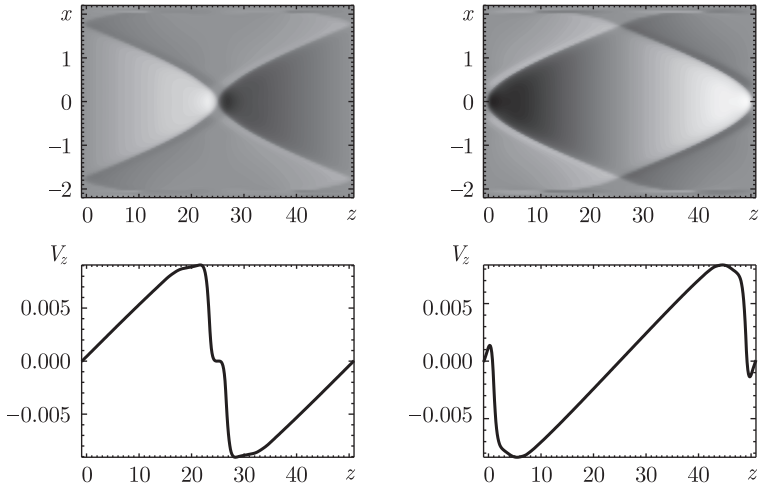

Figure 6. Top panels: spatial profiles of the parallel component of velocity, V_z at $t = 16.82P_2$ (left panels) and V_z at $t = 17.32P_2$ (right panels) for the initial pulse position, $z_0 = L/2$. The corresponding slices of V_z along $x = 0$ are shown in the bottom panels

In this part of the paper we consider the case of the initial pulse launched at $x_0 = 0, z_0 = L/2$. Spatial profiles of the parallel component of velocity, V_z, and its slices along $x = 0$ and $z = L/2$ are shown in Figure 6 at two moments of time. For this pulse position we obtain the first harmonic mode, $n = 2$, excited at $t \approx 4.1P_2$ according to the excitation criterion of Equation (12). Fourier (Figure 9) and wavelet spectra (the latter not shown) yield the wave period of 841.05s, close to the analytical value obtained from Equation (13), *viz.* $P_2 = 847.45$s.

As in the case discussed above, a fast magnetosonic wave is present in the system. Spatial profiles of the perpendicular component of velocity, V_x, are shown in Figure 7 at two given moments of time. The profiles correspond to the opposite phases of a standing fast wave.

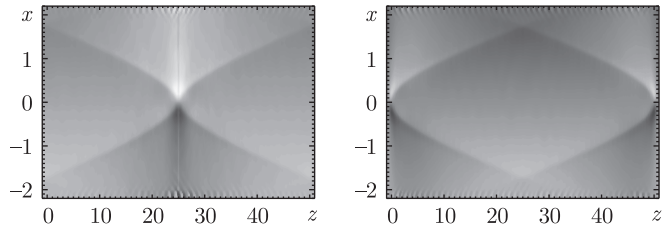

Figure 7. Spatial profiles of the perpendicular component of velocity, V_x, at $t = 16.82P_2$ (left panel) and at $t = 17.32P_2$ (right panel) for initial pulse position $x_0 = 0, z_0 = L/2$

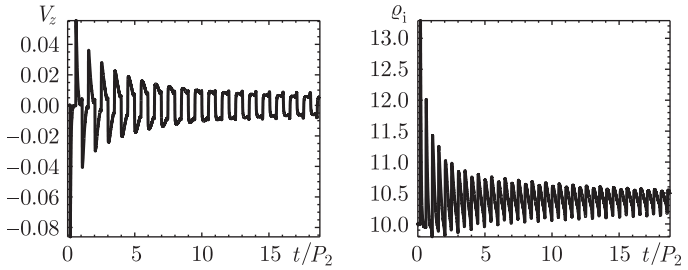

Figure 8. Temporal evolution of velocity, $V_z(x = 0, z = L/4, t)$, (left panel) and mass density, $\varrho_i(x = 0, z = L/4, t)$, (right panel) for the initial pulse position, $x_0 = 0, z_0 = L/2$

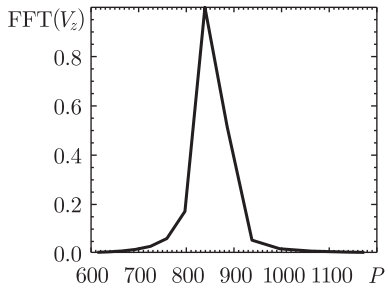

Figure 9. Fourier spectra of $V_z(x = 0, z = L/4, t)$ of Figure 8. The Fourier and wavelet analyses (the latter not shown) yield a wave period of $P_2 = 841.05$ s

Time signatures of parallel velocity, $V_z(x = 0, z = L/4)$, and mass density, $\varrho(x = 0, z = L/4)$, are shown in Figure 8. These curves illustrate the initial stage of slow standing waves' evolution.

4. Summary

We have developed a two-dimensional model of a coronal slab to study numerically standing slow waves. Such waves are triggered by a pulse initially launched in the system, exciting magnetosonic waves among which slow waves are dominant. Depending on the position of this pulse, either fundamental or first harmonic slow modes are generated, associated with standing fast waves. Spectral analysis of time signatures of the magnetosonic waves reveal the presence of several modes, attenuated as a result of energy leakage into the ambient medium. As fast magnetosonic waves are capable of propagation across magnetic field lines, they carry some energy away from the slow modes. Fast magnetosonic waves are coupled as a consequence of a fine value of plasma, β. As a result, slow waves are attenuated further than in

the one-dimensional case discussed by Selwa *et al.* [20]. Our numerical results demonstrate that slow modes are excited faster than in the one-dimensional case. This is a consequence of the presence of fast waves, which distribute energy over a physical system at a speed close to $V_{\rm A}$. The Alfvén speed is greater than the speed of sound, a characteristic speed of slow waves. Interestingly, the excitation time is shorter despite wave periods being longer. More realistic models of slow wave development are being developed.

Acknowledgements

K. Murawski's work was financially supported by a grant from the State Committee for Scientific Research of the Republic of Poland, with KBN grant No. 2PO3D 016 25. The magneto-hydrodynamics code used in this study was developed at the University of Washington by Ogden S. Jones, Uri Shumlak, Scott Eberhardt and Bogdan Udrea and made available to the authors thanks to the sponsorship of the AFOSR program.

References

[1] Nakariakov V M and Verwichte E 2005 *Living Reviews in Solar Physics* **2** 3
[2] Wang T J, Solanki S K, Innes D E, Curdt W and Marsch E 2003 *A&A* **402** L17
[3] Aschwanden M, Fletcher L, Schrijver C and Alexander D 1999 *ApJ* **520** 880
[4] Wang T J and Solanki S K 2004 *A&A* **421** L33
[5] Wang T J, Solanki S K, Curdt W, Innes D E and Dammasch I E 2002 *ApJ* **574** L101
[6] Roberts B, Edwin P M and Benz A O 1984 *ApJ* **279** 857
[7] Mendoza-Briceñ C A, Sigalotti L Di G and Erdélyi R 2003 *Adv. Space Res.* **32** 995
[8] Nakariakov V M, Tsiklauri D, Kelly A, Arber T D and Aschwanden M J 2004 *A&A* **414** L25
[9] Tsiklauri D, Nakariakov V M, Arber T D and Aschwanden M J 2004 *A&A* **422** 351
[10] De Moortel T, Hood A W, Ireland J and Walsh R W 2002 *Solar Phys.* **209** 89
[11] Ofman L 2002 *ApJ* **568** L135
[12] Van Doorsselaere T, Debosscher A, Andries J and Poedts S 2004 *A&A* **424** 1065
[13] Roberts B 2000 *Solar Phys.* **193** 139
[14] Nakariakov V M, Ofman L, DeLuca E E, Roberts B and Davila J M 1999 *Science* **285** 862
[15] Ofman L and Aschwanden M 2002 *ApJ* **576** L153
[16] Ruderman M S and Roberts B 2002 *ApJ* **577** 475
[17] Ofman L and Wang T J 2002 *ApJ* **580** L85
[18] Nakariakov V M, Verwichte E, Berghmans D and Robbrecht E 2000 *A&A* **362** 1151
[19] De Moortel I, Hood A W and Ireland J 2002 *A&A* **381** 311
[20] Selwa M, Murawski K and Solanki S K 2005 *A&A* **436** 701
[21] Mendoza-Briceñ C A, Erdélyi R and Sigalotti L Di G 2004 *ApJ* **605** 493
[22] Roberts B, Edwin P M and Benz A O 1983 *Nature* **305** 688
[23] Murawski K and Roberts B 1993 *Solar Phys.* **143** 89
[24] Jones O S, Shumlak U and Eberhardt D S 1997 *J. Comput. Phys.* **130** 231